

## On stability of jetstreams

A. WIIN-NIELSEN

*Geophysical Department, Niels Bohr Institute for Astronomy, Physics and Geophysics  
University of Copenhagen Haraldsgade 6, 2200 Copenhagen N, Denmark*

(Manuscript received Jan. 18, 1995; accepted in final form March 20, 1995)

### ABSTRACT

The quasi-geostrophic, baroclinic stability problem is solved using vertical structure functions corresponding to a vertical variation of the static stability parameter which is inversely proportional to the square of the pressure. Due to this assumption it is necessary to apply the upper boundary condition at a pressure level different from the outer limit of the atmosphere. While this technique has been used earlier, the emphasis in this paper is on the stability of jet profiles.

Various jet-like profiles of the zonal wind are defined mathematically, and they are used to investigate how the stability depends on the maximum wind, the position of the jet maximum, the sharpness of the jet, and also the position of the upper boundary. A comparison is made with the stability of the advective model for which the stability may be obtained analytically.

From the general, quasi-geostrophic model it is found that a short-wave cut-off exists, while instability exists for all wavelengths larger than the cut-off wavelength, i.e. no long-wave cut-off exists. Smaller instabilities occurs when the maximum wind is around 300 hPa, when the top level is located at 30 hPa, and when the jet profiles are well rounded. A wind profile with "stratospheric easterlies" has about the same stability for Rossby waves of a few thousand kilometers as a profile with westerlies at all levels. However, for very long waves the profile with easterlies is more unstable.

### RESUMEN

El problema de la estabilidad baroclínica cuasi-geostrófica, se resuelve mediante funciones de estructura verticales correspondientes a una variación vertical del parámetro de estabilidad estática que es inversamente proporcional al cuadrado de la presión. Debido a esta suposición es necesario aplicar la condición fronteriza superior en un nivel de presión diferente del límite exterior de la atmósfera. En tanto que esta técnica se ha usado anteriormente, el énfasis en este trabajo es el de la estabilidad de los perfiles del chorro

Se definen matemáticamente varios perfiles que simulan chorros del viento zonal y se amplían para investigar cómo la estabilidad depende del viento máximo; la posición del máximo del chorro; la agudeza del chorro, y también de la posición de la frontera superior. Se hace una comparación con la estabilidad del modelo advectivo para la cual la estabilidad puede obtenerse analíticamente.

A partir del modelo cuasi-geostrófico general, se encuentra que existe una baja segregada de onda corta, mientras que hay estabilidad para todas las longitudes de onda más larga que la correspondiente a la baja segregada, es decir, no existe una baja segregada de onda corta. Ocurren estabilidades menores cuando el viento máximo se halla alrededor de los 300 hPa, cuando el límite superior se localiza a 30 hPa, y cuando los perfiles del chorro están bien redondeados. Un perfil eólico con "vientos estratosféricos del Este" tiene casi la misma estabilidad, para ondas de Rossby de unos pocos miles de kilómetros, como un perfil con vientos ponientes a todos los niveles. Sin embargo para ondas muy largas, el perfil con vientos del Este es más inestable.

## 1. Introduction

The first solution of the baroclinic stability problem was provided by Charney (1947) in his classical paper on the stability of an atmospheric westerly current. The investigation was made using analytical methods. Consequently, the basic state has to be as simple as possible. An atmosphere with a constant lapse-rate in temperature and a linearly increasing wind with height had to be used. A much more general, but still analytical approach to the problem of the stability of internal baroclinic jets was later made by Charney and Stern (1962). Many other studies, too numerous to be mentioned separately, have been made by analytical methods.

Another approach to the same problem was initiated by Green (1960) who solved the eigenvalue problem for the frequency equation by numerical methods. In addition to the major baroclinic instability for waves with a wavelength of a few thousands kilometer he found that also the very long wave exhibited baroclinic instability although with considerably longer e-folding times. While e-folding times of the order of one day are typical for the major baroclinic Rossby waves, the e-folding times for the very long waves are typically 5-7 days. Green's numerical results are in agreement with the results of a theoretical study of the original Charney-problem by Burger (1962, 1966) who found that instabilities exist at all wave-lengths. A different numerical investigation of the atmospheric stability problem was made by Brown (1969) who found the eigen-values by a time-integration to a steady state. This general approach can be applied to a large variety of linear stability problems. The investigations mentioned above apply finite difference methods in the numerical procedures.

The use of vertical structure functions in the solution of the baroclinic instability problem was introduced by Kasahara and Tanaka (1989). They applied a set of normal modes for an especially simple vertical temperature distribution, which corresponds to a vertical distribution of the static stability parameter which is inversely proportional to the square of the pressure. Such a distribution was originally proposed by Gates (1961) based on a data study. Due to the fact that the static stability parameter goes to infinity at the top of the atmosphere it is necessary to apply the upper boundary condition at a finite pressure, different from zero. One of the questions is naturally where the upper level should be selected and how the selection influences the stability. Kasahara and Tanaka (*loc. cit.*) applied the method involving the vertical normal modes to the Charney problem with a linearly increasing wind and to a climatological jet profile typical of 30°N. A weakness in this type of approach is that if the atmospheric parameters, expressed in a series of the vertical structure functions, do not satisfy the same boundary conditions as those used in the design of the vertical modes, there will always be discrepancies close to the boundaries. They used the top boundary condition that the vertical velocity in the p-system should vanish, while the bottom boundary condition was that the vertical velocity in the z-system should vanish corresponding to an Earth without mountains. A linear windprofile is not expressed very accurately close to the boundaries using these structure functions.

Vertical modes, very similar to those described above, have been used by Wiin-Nielsen and Marshall (1990) to investigate the vertical structure of baroclinic, atmospheric waves. In this study the boundary conditions at both the top and the bottom of the atmosphere were that the vertical velocity in the p-system should vanish. The only major consequence of these simplified

boundary conditions is that the external mode, the so-called barotropic component, will be missing. We note that the investigation of the structure of the waves as a by-product can give both the speed and the growth rate of the waves.

A number of years ago Wiin-Nielsen (1967) determined the baroclinic instability of an arbitrary vertical windprofile using the so-called advective model, which is a model with a static stability equal to zero. In this greatly simplified case it is possible to determine both the phase speed and the growth rate from the vertical windprofile. A purpose of this investigation will be to compare the solutions obtained from these two models. The general purpose of this investigation is, however, to calculate the eigen-values of the quasi-geostrophic, baroclinic instability problem for various jet profiles. We shall then be interested in how these eigenvalues are influenced by the shape of the zonal windprofile, the position of the maximum wind, the sharpness of the jet and the location of the top level in the model. For these purposes we shall use the vertical modes as determined by Wiin-Nielsen and Marshall (1990), hereafter called WM.

## 2. The computational scheme

The derivation of the vertical modes is given in detail in Section 3 of WM. It will thus suffice to summarize the properties in this paper. They are solutions to the equation:

$$\frac{d}{dp}[p^2 G] + \lambda^2 G = 0 \quad (2.1)$$

satisfying the boundary condition

$$\frac{dG}{dp} = 0; p = p_T, p = 1 \quad (2.2)$$

where  $p$  is the normalized pressure, i.e. the real pressure divided by the constant pressure  $p_o = 1000$  hPa. The structure equation (2.1) appears when it is assumed that the static stability is given by

$$\sigma = \frac{\sigma_o}{p^2} \quad (2.3)$$

where  $\sigma_o$  is the static stability at  $p = 1$ , i.e. at the surface. The solutions are:

$$G_n(p) = \frac{D(n)}{\sqrt{p}} \left[ \sin\left(n\pi \frac{\xi}{\xi_T}\right) - 2\mu(n) \cos\left(n\pi \frac{\xi}{\xi_T}\right) \right] \quad (2.4)$$

where

$$\xi = -\ln(p)$$

$$\xi_T = -\ln(p_T)$$

$$D(n) = \left[ \frac{2}{(1 + 4\mu(n)^2)\xi_T} \right]^{1/2} \quad (2.5)$$

$$\mu(n)^2 = \lambda(n)^2 - \frac{1}{4}$$

giving

$$\lambda(n)^2 = \frac{1}{4} + \left[ \frac{n\pi}{\xi_T} \right]^2 \quad (2.6)$$

The functions  $G_n(p)$  form an orthogonal, normalized set over the interval  $p_T$  to 1 as shown in WM. The basic equation for quasi-geostrophic flow expresses the conservation of the Charney vorticity in the horizontal, nondivergent flow. The Charney vorticity is:

$$Q = f + \nabla^2 \Psi + \frac{\partial}{\partial p} \left( \frac{f_o^2}{\sigma_o p_o^2} \frac{\partial \Psi}{\partial p} \right) \quad (2.7)$$

The basic equation is therefore:

$$\frac{\partial Q}{\partial t} + u \frac{\partial Q}{\partial x} + v \frac{\partial Q}{\partial y} = 0 \quad (2.8)$$

This general equation could be used to formulate a mixed barotropic-baroclinic problem. However, we shall consider the classical, purely baroclinic stability problem assuming that the zonal current  $U = U(p)$  varies with pressure only. Similarly, we shall assume that the perturbation streamfunction  $\psi = \psi(x, p, t)$  is given by

$$\psi = \Psi(p) \exp(ik(x - ct)) \quad (2.9)$$

where  $\Psi(p)$  is the complex amplitude,  $k$  the wave number,  $c$  the complex wavespeed,  $x$  the distance in the zonal direction and  $t$  the time. We shall next formulate the general eigen-value problem. Using the assumptions made above and following the usual rules for creating a linear problem we find that the linear perturbation equation is:

$$(U - c) \left[ \frac{d}{dp} \left( \frac{f_o^2}{\sigma_o p_o^2} p^2 \frac{d\Psi}{dp} \right) - k^2 \Psi \right] + \left[ \beta - \frac{d}{dp} \left( \frac{f_o^2}{\sigma_o p_o^2} p^2 \frac{dU}{dp} \right) \right] \Psi = 0 \quad (2.10)$$

The problem is to determine the eigen-value ( $c$ ) from the frequency equation (2.10). To this end we express  $U(p)$  and  $\psi(p)$  in series of the structure functions, where the vertical mean has been removed from  $U(p)$ . We may thus write:

$$U(p) = \sum_{r=1}^N U(r) G_r(p)$$

$$\Psi(p) = \sum_{r=1}^N \Psi(r) G_r(p) \quad (2.11)$$

The series (2.11) are inserted in the frequency equation (2.10). To find the equation for a single amplitude  $\psi(n)$  we multiply the resulting equation by  $G_n(p)$  and integrate from  $p_T$  to 1 with respect to  $p$ . Making use of the orthogonality properties we arrive at the equation:

$$-\left[\frac{C_R}{1 + \gamma^2 \lambda(n)^2} + c\right] \Psi(n) + \sum_{s=1}^N \sum_{r=1}^N \frac{1 + \gamma^2 (\lambda(s)^2 - \lambda(r)^2)}{1 + \gamma^2 \lambda(n)^2} U(r) I(r, s, n) \Psi(s) = 0 \quad (2.12)$$

In (2.12) we have introduced the following notations:

$$C_R = \frac{\beta}{k^2}; \gamma^2 = \frac{q^2}{k^2}; q^2 = \frac{f_o^2}{\sigma_o p_o^2} \quad (2.13)$$

The set of equations (2.12) for  $n = 1, 2, \dots, N$  will be recognized as a standard eigen-value problem expressed in a matrix since (2.12) gives the rules for the determination of all elements in the matrix. The notation  $I(r, s, n)$  stands for the interaction integral:

$$I(r, s, n) = \int_{p_T}^1 G_r(p) G_s(p) G_n(p) dp \quad (2.14)$$

It is seen that  $I$  is independent of the order of  $r, s$  and  $n$ .  $I$  is a measure of the contribution to component  $n$  from all pairs  $(r, s)$  of the spectrum. We recall that the windprofile  $U(p)$  is given in the stability problem. The amplitudes  $U(n)$  are obtained in the usual way, i.e.

$$U(n) = \int_{p_T}^1 U(p) G_n(p) dp \quad (2.15)$$

For a given profile  $U(p)$  and a given wavelength we may summarize the computational scheme as follows:

1.  $U(n)$  is calculated for all  $n$  from (2.15)
2. All interaction integrals are calculated.
3. A standard eigen-value computer routine is used to determine the eigen values of the system (2.12).
4. The eigen-value with the largest positive imaginary value indicates the maximum instability for the given parameters.

### 3. Results

The following rather flexible specification of  $U(p)$  has been used:

$$U(p) = U_m \frac{(p - p_T)^a (1 - p)^b}{(p_m - p_T)^a (1 - p_m)^b} \quad (3.1)$$

It is similar to the formula used by Wiin-Nielsen (1967) and can be used to investigate the properties of the windprofile on the stability of the zonal flow. (3.1) has a maximum value of  $U_m$  at  $p = p_m$  if  $a$  and  $b$  are related by

$$b = \frac{1 - p_m}{p_m - p_T} a \quad (3.2)$$

Example 1: In this example we have selected  $a = 2$  and  $p_m = 1/4$  giving  $b = 7.5$ . Since  $U(1) = 0$ ,  $U_m$  is also a measure of the averaged windshear below the maximum. The eigen-value problem has been solved with  $U_m$  varying from 0 to 100 m per s for wavelengths up to 28000 km, corresponding to wave number 1 in mid-latitudes. The results for  $0 < L < 14000$  km are shown in Figure 1 where isolines have been drawn for the e-folding time, measured in days. In each case we have selected only the most unstable mode. It is observed that a short wave cut-off exists. It is located between 1500 and 2000 km. The maximum instability is found around 3500 km, and  $T_e$  reaches a minimum of about 1/2 day at the excessive value of  $U_m = 100$  m per s. The diagram continues in Figure 2 for  $14000 < L < 28000$  km. Although curves for the e-folding times are drawn up to 10 days only, we emphasize that an instability exists in all points for  $U_m \geq 5$  m per s, but the e-folding times become very large for large  $L$ . For example for  $L = 28000$  km and  $U_m = 5$  we find  $T_e = 45.5$  days. For more realistic values of the maximum wind the e-folding time is about 2 weeks.

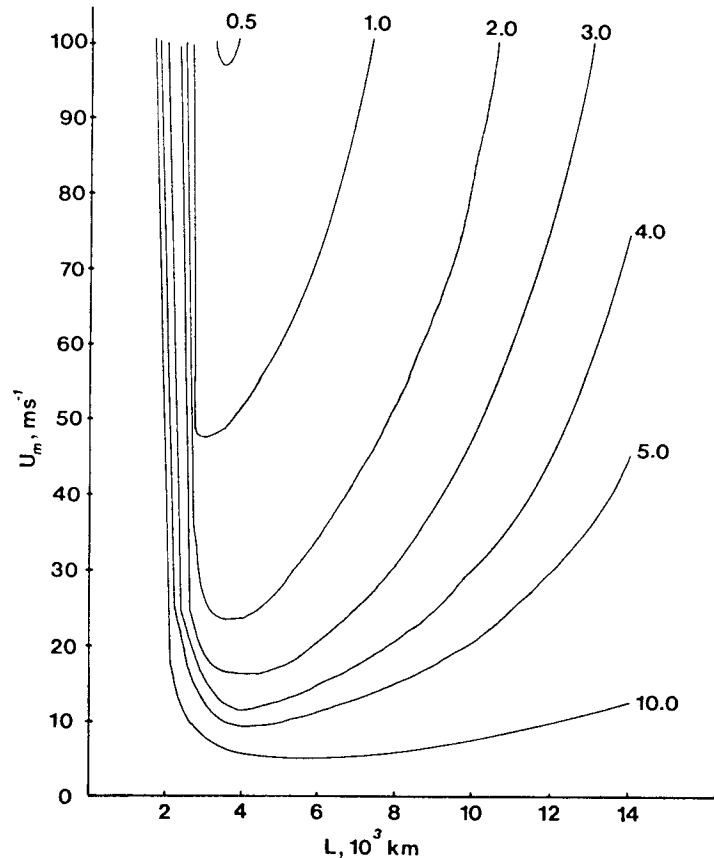


Fig. 1. The e-folding times in days as a function of the wavelength and the maximum windspeed for a zonal current specified by eq. (3.1) for  $a = 2$ ,  $p_m = 1/4$ .

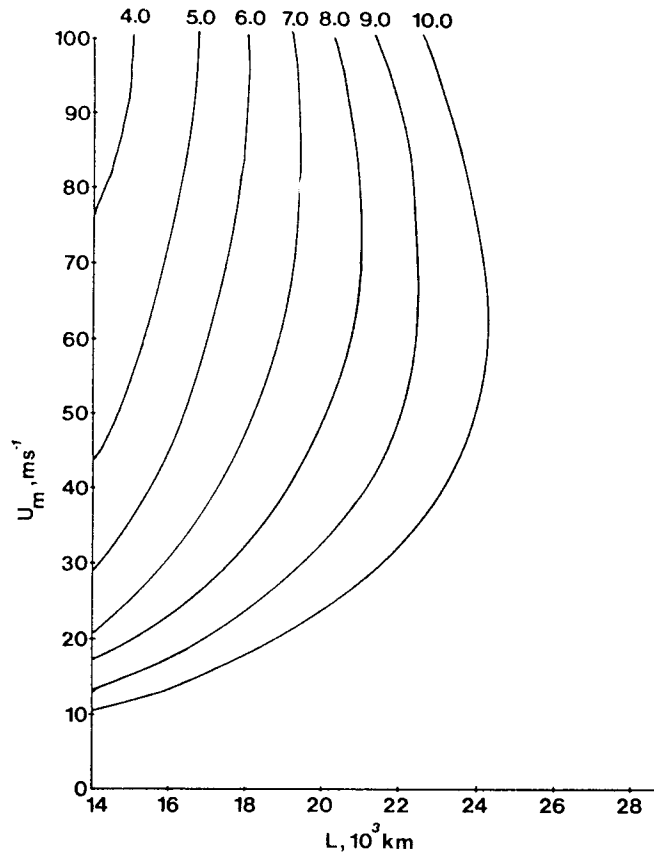


Fig. 2. A continuation of Figure 1 for wavelengths larger than 14000 km.

Figure 3 shows three wind profiles using (3.1) having the same value of  $U_m$ , but with maxima at  $p_m = 0.15, 0.25$  and  $0.35$ .  $a = 2$  for all cases, but  $b$  has in each case been determined from (3.2). The e-folding times have been computed for a large number of profiles of the type shown in Figure 3 with  $p_m$  varying from 0.1 to 0.4 for  $L = 3500$  km. The results are shown in Figure 4 which indicates that the accuracy of the determination of the e-folding times is not very large since we would undoubtedly expect a smoother curve. However, it is clear that the least unstable windprofile should have its maximum between  $p_m = 0.25$  and  $p_m = 0.35$  which is close to the level where the observed jets are located.

An undesirable feature of the present formulation is that a "lid" at  $p_T > 0$  has to be used in all calculations. Earlier calculations by Kasahara and Tanaka (1989) used  $p_T = 0.1$  (100 hPa). Since the e-folding times may vary with  $p_T$  we have used two different maximum speeds (40 and 60 m per s for  $U_m$ ) and  $L = 3500$  km to calculate  $T_e$  when  $p_T$  is varying from 0.01 to 0.1. In each case we had  $a = 2$  and  $p_m = 0.25$ . Figure 5 shows that the largest e-folding time is found for  $p_T = 0.03$  (30 hPa) for both cases. We have also investigated the influence of the sharpness of the jet on the stability. We used  $p_m = 0.25$ , varied  $a$  and determined  $b$  from (3.2). Large values of  $a$  mean a very sharp jet maximum, but also much smaller windspeeds away from the maximum having in these experiments a constant value. Figure 6 shows that the larger values of  $T_e$  occur for small values of  $a$ , or, in other words, instability increases with the sharpness of the jet.

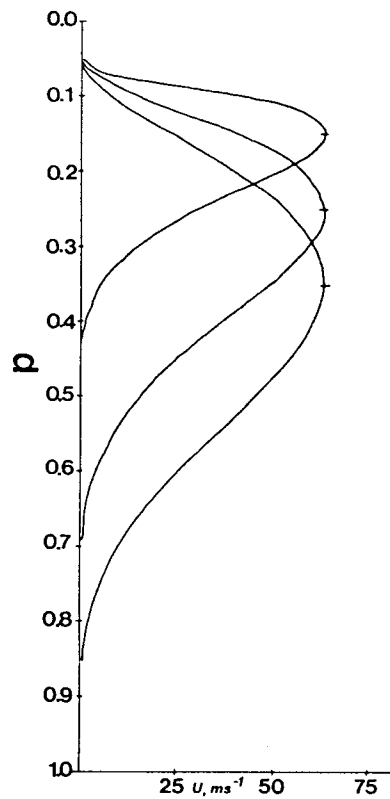


Fig. 3. Various zonal jet stream profiles with maxima at 0.15, 0.25 and 0.35, but with the same maximum speed,  $a = 2$ .

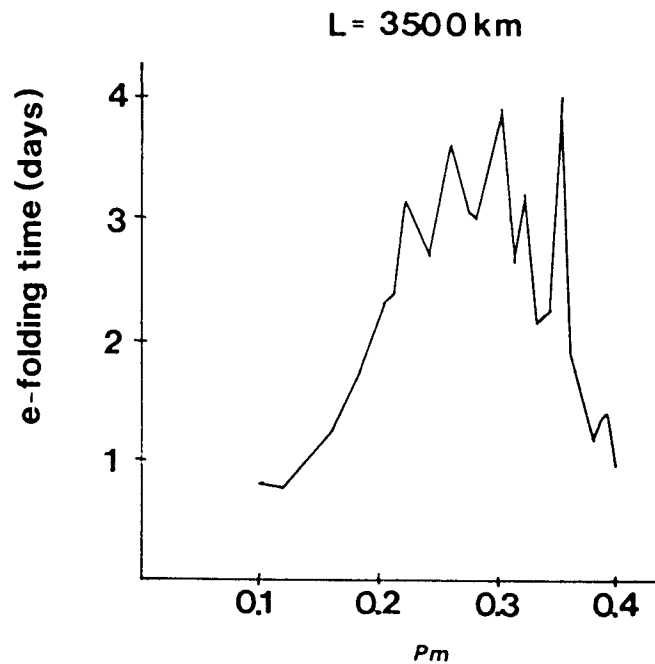


Fig. 4. The e-folding time (in days) as a function of the position ( $pm$ ) of the maximum wind for a single horizontal wavelength of 3500 km.



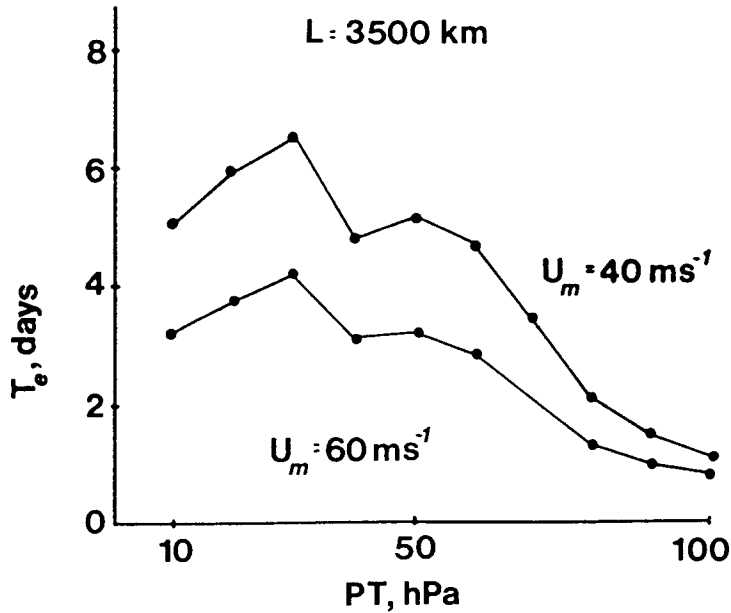


Fig. 5. The e-folding time (in days) as a function of the position of the top level ( $p_T$ ) for  $L = 3500$  km and for the two maximum windspeeds,  $U_m = 40$  m per s and  $U_m = 60$  m per s.

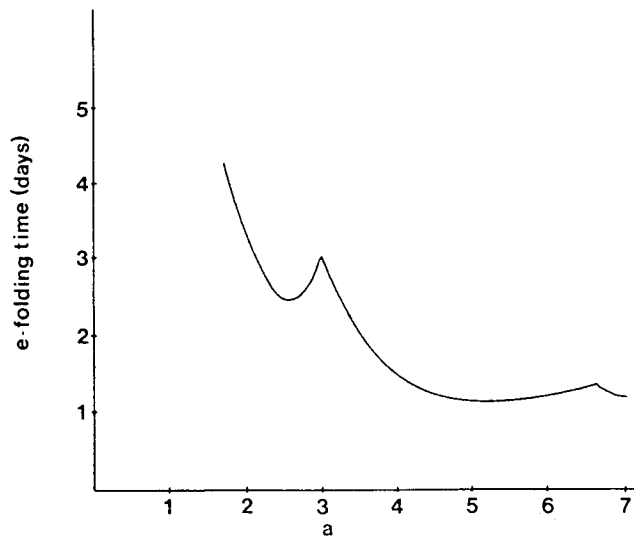


Fig. 6. The e-folding time (in days) as a function of the sharpness of the jet maximum as measured by the parameter  $a$ .

Example 2: We shall compare the stability in the advective model with the present model. The solution for the phase speed in the advective model is according to Wiin-Nielsen (1967):

$$c = U_m - 1/2C_r \pm \left(\frac{1}{4} C_r^2 - I_d\right)^{1/2} \quad (3.3)$$

where  $U_m$  is the vertically averaged wind and  $I_d$  is the integral:

$$I_d = \int_0^1 U_T^2 dp; U_T = U - U_m \quad (3.4)$$

The calculations of the e-folding time for the advective model is thus straightforward. Using the same windprofiles as given in (3.1) we note that  $I_d$  for this case is:

$$I_d = \left[ \frac{(2a)!(2d)!}{(2a+2b+1)!} - \left( \frac{a!b!}{(a+b+1)!} \right)^2 \right] \frac{U_m^2}{p_m^{2a}(1-p_m)^{2b}} \quad (3.5)$$

The e-folding time for the advective model is shown in Figure 7. A comparison between this figure and Figure 1 shows that the advective model has no short wave cut-off. As a matter of fact the e-folding time goes to zero when the wavelength goes to zero, the so-called ultraviolet catastrophe. On the other hand, the advective model has a long wave cut-off which is due to the beta effect, and, finally, the advective model is much more unstable than the more general model used in example 1. There are differences of an order of magnitude in some cases.

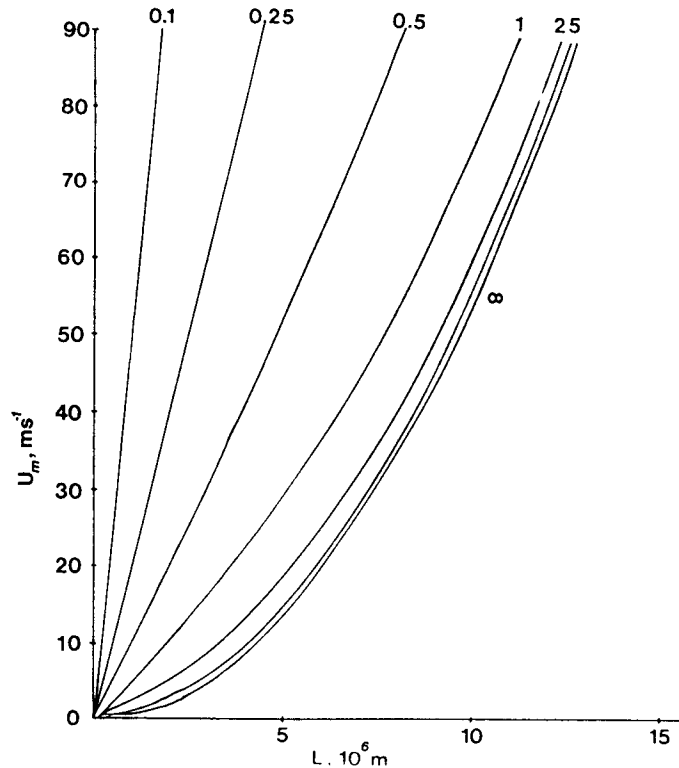


Fig. 7. The stability of the advective model shown in the same way as in Figure 1.

Example 3: While windprofile defined by (3.1) has westerlies at all levels, the real atmosphere has easterlies on top of the westerlies. To design an example with the observed features we define for  $p_T \leq p \leq p_m$  that

$$U(p) = U_m \frac{(p-p_T)^2(p-p_s)}{(p_m-p_T)^2(p_m-p_s)} \left[ 1 + \frac{3p_m - 2p_s - p_T}{(p_m-p_T)(p_m-p_s)} (p_m-p) \right] \quad (3.6)$$

The profile given in (3.6) satisfies the conditions that its maximum ( $U_m$ ) occurs at  $p = p_m$ ,

that it has a zero at a level  $p_s$  in the stratosphere, and that both the value and the derivative at  $p = p_T$  are zero. For the remaining part of the windprofile ( $p_m \leq p \leq 1$ ) we may use

$$U(p) = U_m \frac{(1-p)^2}{(1-p_m)^2} \left(1 + 2 \frac{p-p_m}{1-p_m}\right) \quad (3.7)$$

The profile described by the two expressions in (3.6) and (3.7) is shown in Figure 8. It has been used to calculate the stability using the same procedure as in example 1. The results are displayed in Figure 9. The main features of the curves in Figure 1 and Figure 2 can be found in Figure 9. A short-wave cut-off is found again although at slightly smaller wavelengths than in the previous case. For larger wavelengths we find instability in all points in which the calculation has been made. A closer inspection of the curves shows, however, that the present case in general results in a larger degree of instability in corresponding points for the longer waves. We may thus conclude that the introduction of easterlies in the top part of the model has a destabilizing effect.

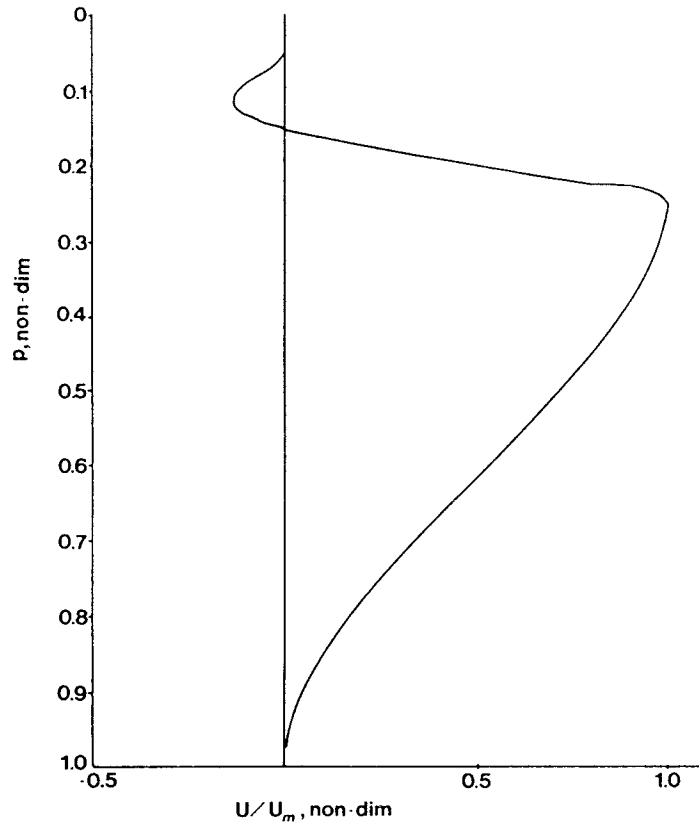


Fig. 8. The windprofile ( $U/U_m$ ) containing high level easterlies.

A number of additional calculations have been performed to investigate if the conclusions, drawn in this section from the numerical experiments, are sensitive to small changes in the parameters. This does not seem to be the case.

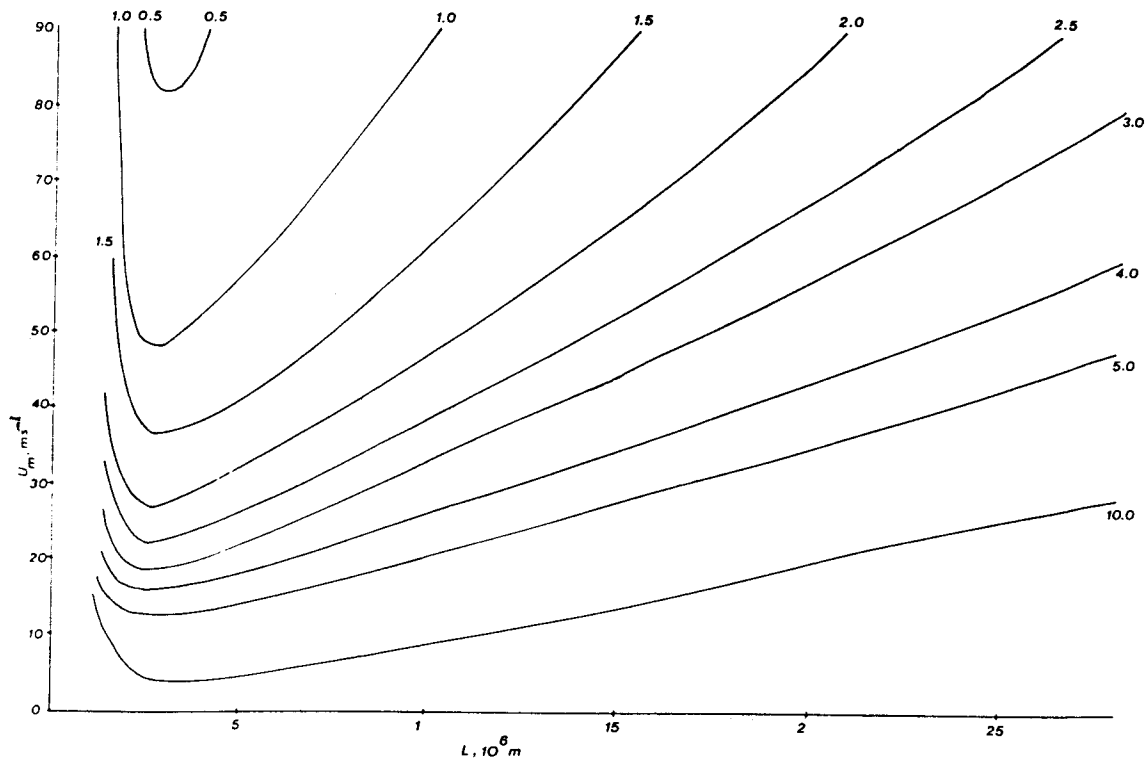


Fig. 9. The stability diagram for the windprofiles containing easterly flow in the upper part of the atmosphere as displayed in Figure 8.

#### 4. Concluding remarks

The main purpose of the present investigation has been to explore the stability properties of jet streams in the atmosphere. For this purpose a number of rather flexible mathematical expressions have been designed. By changing the parameters it is possible to change the strength of the flow, the position and the sharpness of its maximum, and the location of the upper lid. Other examples, containing both westerlies and easterlies, have been used.

Eigenvalues are determined for all cases using the vertical structure functions designed as an orthogonal, normalized set, determined for a distribution of the static stability parameter that is inversely proportional to square of the pressure. The main results are that the advective model is too simple to display the real stabilities of the zonal flow, that the instability increases with the strength and the sharpness of the jet, while the positions of the jet and the upper boundary have minor influences on the stability. A vertical wind profile with stratospheric easterlies result in somewhat larger instabilities for the longer waves, but practically no change for the shortest baroclinic waves.

The vertical structure functions applied in this study are probably good approximations although they are derived for a special stratification of the atmosphere. Generalizations can be made, but the resulting functions are far from efficient in describing the processes in the troposphere since the zeroes of the more general functions are located mainly in the upper part of the atmosphere.

## REFERENCES

- Brown, J. A., Jr., 1969. A numerical investigation of hydrodynamic instability and energy conversions in the quasi-geostrophic atmosphere, Part I and Part II, *Jour. of Atmos. Sci.*, **26**, 352-375.
- Burger, A. P., 1962. On the non-existence of critical wavelengths in a continuous baroclinic instability problem, *Jour. of Atmos. Sci.*, **19**, 31-38.
- Burger, A. P., 1966. Instability associated with the continuous spectrum in a baroclinic flow, *Jour. of Atmos. Sci.*, **23**, 272-277.
- Charney, J. G., 1947. The dynamics of long waves in a baroclinic westerly current, *Jour. of Meteor.*, **4**, 135-162.
- Charney, J. G. and M. E. Stern, 1962. On the stability of internal baroclinic jets in a rotating atmosphere, *Jour. of Atmos. Sci.*, **19**, 159-172.
- Gates, W. L., 1961. Static stability measures in the atmosphere, *Jour. of Meteor.*, **18**, 526-533.
- Green, J. S. A., 1960. A problem in baroclinic instability, *Quart. Jour. of the Roy. Met. Soc.*, **86**, 237-251.
- Kasahara, A. and H. C. Tanaka, 1989. Application of vertical normal mode expansion to problems of baroclinic instability, *Jour. of Atmos. Sci.*, **46**, 489-510.
- Wiin-Nielsen, A., 1967. On baroclinic instability as a function of the vertical profile of the zonal wind, *Mon. Wea. Rev.*, **95**, 733-739.
- Wiin-Nielsen, A. and H. Marshall, 1990. On the structure of transient atmospheric waves, Part III, *Atmósfera*, **3**, 73-109.